

Synthesis and Structural Characterization of Main Group 15 Organometallics R_3M and $R(Ph)_2P(=N-Ar)$ ($M = P, Sb, Bi$; $R = \text{phenanthrenyl}$; $Ar = 2,6\text{-}i\text{-Pr}_2\text{-C}_6\text{H}_3$)

Eun Ji Lee, Jin Seok Hong, Tae-Jeong Kim,* Youngjin Kang,^{†,*} Eun Me Han,[‡]
Jae Jung Lee,[‡] Kihyung Song,[§] and Dong-Uk Kim[#]

Department of Applied Chemistry, Kyungpook National University, Daegu 702-701, Korea. *E-mail: tjkim@knu.ac.kr

[†]Division of Science Education, Kangwon National University, Chun Cheon 200-701, Korea

[‡]Faculty of Applied Chemical Engineering, Chonnam National University, Gwangju 500-757, Korea

[§]Department of Chemistry, Korea National University of Education, Chongwon, Chungbuk 363-791, Korea

[#]Department of Science Education, Daegu National University of Education, Daegu 705-715, Korea

Received September 22, 2005

New group 15 organometallic compounds, $M(\text{phenanthrenyl})_3$ ($M = P$ (**1**), Sb (**2**), Bi (**3**)) have been prepared from the reactions of 9-phenanthrenyllithium with MCl_3 . A reaction of 9-(diphenylphosphino)phenanthrene with 2,6-diisopropylphenyl azide led to the formation of $(\text{phenanthrenyl})(Ph)_2P=N-(2,6\text{-}i\text{-Pr}_2\text{C}_6\text{H}_3)$ (**4**). The crystal structures of **2** and **4** have been determined by single-crystal X-ray diffractions, both of which crystallize with two independent molecules in the asymmetric unit. Compound **2** shows a trigonal-pyramidal geometry around the Sb atom with three phenanthrenyl groups being located in a screw-like fashion with an approximately C_3 symmetry. A significant amount of $CH\cdots\pi$ interaction exists between two independent molecules of **4**. The phosphorus center possesses a distorted tetrahedral environment with P-N bond lengths of 1.557(3) Å (P(1)-N) and 1.532(3) Å (P(2)-N), respectively, which are short enough to support a double bond character. One of the most intriguing structural features of **4** is an unusually diminished bond angle of C-N-P, attributable to the hydrogen bonding of N(1)-H(5A) [*ca.* 2.49 Å] between two adjacent molecules in crystal packing. The compounds **1-3** show purple emission both in solution and as films at room temperature with emission maxima (λ_{max}) at 349, 366, and 386 nm, respectively, attributable to the ligand-centered $\pi \rightarrow \pi^*$ transition in phenanthrene contributed by the lone pair electrons of the Gp 15 elements. Yet the nature of luminescence observed with **4** differs in that it originates from π (diisopropylbenzene)- π^* (phenanthrene) transitions with the $p\pi$ -contribution from the nitrogen atom. The emission maximum of **4** is red-shifted ranging 350-450 nm due to the internal charge transfer from the phenanthrenyl ring to the *N*-arylamine group as deduced from the *ab initio* calculations.

Key Words : Group 15 organometallics, $M(\text{phenanthrenyl})_3$, $(\text{Phenanthrenyl})(Ph)_2P=NAr$

Introduction

Luminescent organic and organometallic compounds are currently of intense research interest due to their potential applications in sensor technologies and photochemical and electroluminescent devices.¹⁻³ In particular, special emphasis has recently been focused on the development of phosphors based on transition metals and main-group complexes for applications in organic light-emitting devices (OLEDs) because they are known to enhance overall device efficiency through the use of phosphorescence due to MLCT transition, in contrast to the emissions of most organic compounds dominated by fluorescence.⁴ Heavy metal centers introduced into the organic ligands play a key role in singlet-triplet state mixing and, hence phosphorescent emission (*the heavy atom effect*).⁴ The most representative organotransition metal complexes are cyclometalated Ir(III) and Pt(II) complexes of the types $(C^{\wedge}N)_3Ir$, $(C^{\wedge}N)_2Ir(\text{diketonate})$, and $(C^{\wedge}N)Pt(\text{diketonate})$, where $C^{\wedge}N$ represents cyclometalating aromatic chelates (*e.g.*, 2-arylpyridine).^{4,5} Here cyclometalation has become an attractive synthetic prototype to enhance conformational stability and rigidity thus minimizing the energy

loss by thermal vibrational decay.⁶ A serious drawback of these transition-metal ions, however, is that they very often quench the emission from the ligand due to the presence of the incomplete $5d$ shell.

An alternative approach to overcome these difficulties is the use of heavy main-group elements, since they not only exhibit strong spin-orbital coupling but also do not interfere with the electronic transitions of the ligand due to the closed shell electronic configuration: $(n-1)d^{10}ns^2np^5nd^0$. Furthermore, the availability of the unoccupied nd orbitals of the heavy main-group elements allows valence expansion and the accommodation of multidentate ligands. These advantages have fully been exploited for the first time by Wang's group, consequently resulting in a great number of blue phosphorescent groups 13-15 organometallics that contain terminal aryl ligands functionalized by 7-azaindolyl or 2,2'-dipyridylamino groups.⁷ The same group has demonstrated that the heavier main-group elements drastically enhance phosphorescent emission of the ligands.

These results encourage not only further investigation of the use of other luminescent aryl ligands but also the development of new types of organometallics comprising

heavier main-group elements. Intrigued by the work of Wang described above and motivated by our continued effort on the design and the synthesis of novel luminescent organometallic complexes for applications in OLEDs,⁸ we have investigated a series of organometallic compounds of group 15 of the types R_3M and $RPh_2M(=N-Ar)$ ($M = P, Sb, Bi$; $R = 9$ -phenanthrenyl; $Ar = 2,6$ - iPr_2 - C_6H_3) as potential application to OLED. In connection with the investigation of the latter type compound incorporating the $P=N-Ar$ unit, it is worth mentioning that phosphorus has become an attractive candidate for replacement of carbon in $p\pi-p\pi$ conjugated materials due to its similar electronegativity; indeed, phosphorus has often been referred to as a “carbon copy”,⁹ and calculations predict similar conjugative abilities for phosphorus and carbon in olefinic type bonds.¹⁰ Recently, poly(p -phenylenephosphaalkene)s have been prepared and shown to exhibit properties expected for conjugation.¹¹ Herein we report their synthesis, characterization, and photophysical properties.

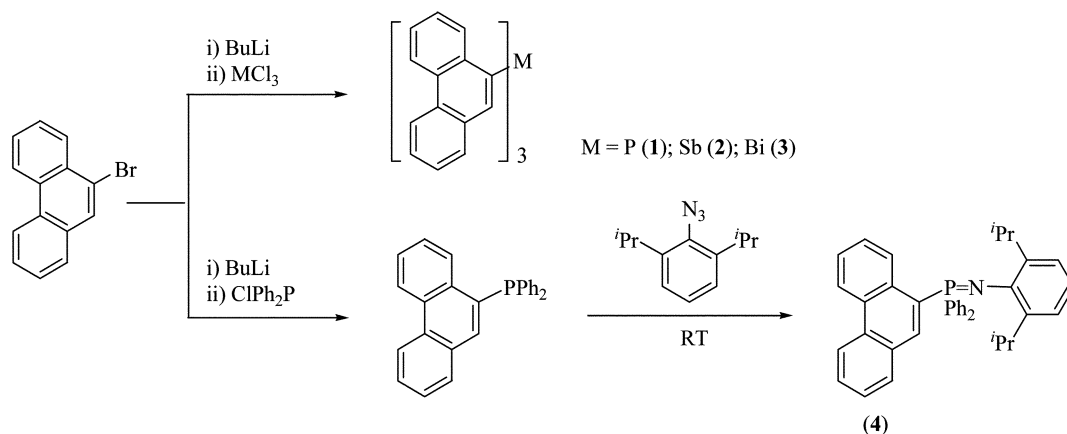
Results and Discussion

Synthesis and Characterization. Scheme 1 shows the preparative methods leading to the formation of our target compounds **1-4**. Namely, addition of MCl_3 ($M = P, Sb, Bi$) to phenanthrenyl lithium, prepared from the reaction of 9-bromophenanthrene with n -BuLi, gives **1-3** as off-white solids after standard workup and crystallization from a mixture of dichloromethane and hexane. A pale yellow crystalline solid of **2** suitable for X-ray diffraction analysis was grown by slow diffusion of hexane into the dichloromethane solution of **2**. Although all compounds are stable indefinitely in the solid state, yet decompose slowly in solution over a period of several days. The preparation of an iminophosphorane **4** requires initially the synthesis and isolation of 9-(diphenylphosphino)phenanthrene, followed by treatment with 2,6-bis(diisopropyl)benzoyl azide. Again yellow single crystals suitable for X-ray diffraction analysis were obtained by slow diffusion of hexane into the dichloromethane solution of **4**.

Structural confirmations of new compounds come from

spectroscopic (NMR & GC/MS) and micro-analytical techniques. For instance, the formation of **1** can be easily recognized by the characteristic down-field singlet (-28.7 ppm) on ^{31}P NMR, in addition to the signals assignable to the phenanthrenyl protons on 1H NMR. As for **2** and **3**, virtually the same 1H NMR patterns as for the aromatic ring protons are observed, which makes their structural identification quite straightforward. The formation of the iminophosphorane bond in **4** can be confirmed by the presence of a low-field ^{31}P NMR singlet (-4.04 ppm) appearing from the phosphorane group. Further, its 1H NMR shows a typical doublet (0.66 ppm, $J = 6.6$ Hz) arising from the twelve equivalent protons of a pair of isopropyl groups.

The structures of **2** and **4** were unambiguously established by single-crystal X-ray diffraction analyses. Selected bond lengths and angles are presented in Table 2; refinement and structure-solution data can be found in the experimental section. Interestingly, both compounds crystallize with two independent molecules in a unit cell. For compound **2**, the overall geometries of two molecules do not differ significantly, nor exhibit short intermolecular contacts such as $\pi-\pi$ stacking. The central Sb atom adopts a trigonal-pyramidal coordination geometry as shown in Figure 1. The three phenanthrenyl groups are located in a screw-like fashion to reveal an approximately C_3 symmetry. Both the Sb(1)-C bond lengths of $2.154(4)$ Å– $2.165(3)$ Å and the C-Sb(1)-C bond angles of [$94.12(12)^\circ$ – $98.12(12)^\circ$] are within the range reported for related organophosphorus(III) compounds with phenyl moieties. The sum of bond angles around Sb(1) is 290.34° , while the value is slightly reduced in the case of Sb(2) which gives rise to 286.79° . Unusually small angles such as these as compared with those found in the phosphorus analogues $P(aryl)_3$, represent a well-documented observation that the C-M-C bond angles in the $M(aryl)_3$ series ($M = P, Sb, Bi$; $R = aryls$) decrease as going down in the same group of the periodic table.⁷ Such a trend as mentioned above has been explained in terms of the increased s -orbital character in the hybrid orbitals of heavier elements such as SbR_3 as compared with PR_3 . The phosphorus center in **4** possesses a distorted tetrahedral geometry with an average bond length (P-C) of 1.815 Å and an aver-



Scheme 1

Table 1. Summary of crystallographic data for **2** and **4**

	2	4
empirical formula	C ₄₂ H ₂₇ Sb•0.5CH ₂ Cl ₂	C ₃₈ H ₃₆ NP
fw	695.85	537.65
<i>T</i> (°K)	173(2)	173(2)
radiation, λ (Å)	Mo Kα 0.71073	Mo Kα 0.71073
crystal system	triclinic	monoclinic
space group	P-1	C2/c
<i>a</i> (Å)	9.6229(4)	38.6653(18)
<i>b</i> (Å)	17.8748(7)	9.8651(5)
<i>c</i> (Å)	19.6841(8)	31.7316(14)
α (deg)	87.3800(10)	90
β (deg)	76.0890(10)	97.8460(10)
γ (deg)	76.1940(10)	90
<i>V</i> (Å ³)	3191.3(2)	11990.3(10)
<i>Z</i>	4	16
<i>D</i> _{calcd} (g cm ⁻³)	1.448	1.191
μ (mm ⁻¹)	0.978	0.119
F(000)	1404	4576
cryst size (mm ³)	0.50 × 0.30 × 0.20	0.3 × 0.2 × 0.1
2θ range (deg)	2.14–56.58	2.12–56.62
data collected: <i>h</i> ; <i>k</i> ; <i>l</i>	–12, 12; –23, 19; –24, 25	–41, 50; –12, 10; –42, 41
reflections collected	20487	37759
independent reflections	14326 [R(int) = 0.0173]	14190 [R(int) = 0.1203]
completeness to θ = 28.29°	90.4%	95.0%
GOF	1.072	0.977
<i>R</i> indices (<i>I</i> > 2σ(<i>I</i>)) ^a	<i>R</i> ₁ = 0.0359; <i>wR</i> ₂ = 0.0984	<i>R</i> ₁ = 0.0747; <i>wR</i> ₂ = 0.1789
largest diff. peak and hole (e/Å ³)	2.277, –1.047	0.681, –0.764

Table 2. Selected bond lengths (Å) and angles (deg) for **2** and **4**

2			
Sb(1)–C(1)	2.165(3)	Sb(2)–C(43)	2.162(3)
Sb(1)–C(15)	2.154(3)	Sb(2)–C(57)	2.157(3)
Sb(1)–C(29)	2.151(4)	Sb(2)–C(71)	2.158(3)
C(1)–Sb(1)–C(15)	98.10(12)	C(43)–Sb(2)–C(57)	97.77(12)
C(1)–Sb(1)–C(29)	94.12(12)	C(43)–Sb(2)–C(71)	93.89(12)
C(15)–Sb(1)–C(29)	98.12(12)	C(57)–Sb(2)–C(71)	95.13(12)
4			
P(1)–N(1)	1.557(3)	P(2)–N(2)	1.532(3)
P(1)–C(15)	1.806(4)	P(2)–C(53)	1.807(4)
P(1)–C(21)	1.810(3)	P(2)–C(59)	1.829(4)
P(1)–C(1)	1.830(3)	P(2)–C(39)	1.830(4)
N(1)–C(27)	1.427(4)	N(2)–C(65)	1.387(4)
N(1)–P(1)–C(15)	109.14(16)	N(2)–P(2)–C(53)	109.72(18)
N(1)–P(1)–C(21)	113.81(16)	N(2)–P(2)–C(59)	117.35(17)
C(15)–P(1)–C(21)	107.56(16)	C(53)–P(2)–C(59)	106.23(16)
N(1)–P(1)–C(1)	117.38(15)	N(2)–P(2)–C(39)	115.14(17)
C(15)–P(1)–C(1)	102.86(15)	C(53)–P(2)–C(39)	104.67(16)
C(21)–P(1)–C(1)	105.19(16)	C(59)–P(2)–C(39)	102.61(16)
C(27)–N(1)–P(1)	125.6(2)	C(65)–N(2)–P(2)	147.8(3)

age bond angle (C–P–C) of 110.17. The P–N bond lengths at P(1) and P(2) are 1.557(3) Å and 1.532(3) Å, respectively.

These values are sufficiently short to support a double bond character. Interestingly, a significant amount of CH---π (C18H60 : 2.802 Å and C18H60 : 2.873 Å) interaction exists between two adjacent molecules of **4**. A further interesting structural feature of **4** is that the bond angle of C(27)–N(1)–P(1) [125.6(2)°] is considerably smaller than that of C(65)–N(2)–P(2) [147.8(3)°]. The diminished bond angle can be ascribed to the hydrogen bonding of N(1)–H(5A) [*ca.* 2.49 Å] between two adjacent molecules in the crystal packing as shown in Figure 2. Finally, in connection with **4**, one might expect a cyclometallation reaction involving the =N–Ar group and the C-10 atom of phenanthrene.¹² To our disappointment, however, many attempts to obtain such cyclometallated products employing various transition metal complexes proved futile, leading only to the formation of unidentified black precipitates.

Photophysical Properties. The UV/Vis absorption spectra of **1–4** were taken in CH₂Cl₂ and their λ_{max} values collected in Table 3. In Figure 3 are also shown absorption and emission spectra of **2** and **4**. All compounds except **4** have two characteristic absorption bands in common: intense bands at shorter wavelengths (λ_{max} 246–265 nm; ε = 180080–499330 M⁻¹cm⁻¹) are attributable to the phenanthrene-based π–π* transitions, and weaker shoulders at longer wavelengths (λ_{max} 297–303 nm; ε = 44740–126330 M⁻¹cm⁻¹) to the charge transfer from the lone pair electrons to the phenanthrene ligand.¹³ The absorption maxima move toward

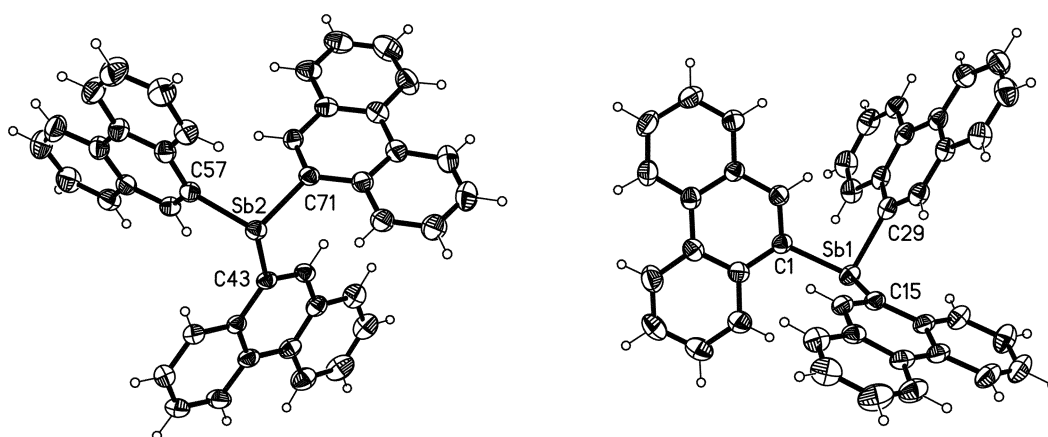


Figure 1. Molecular structure of **2** along with atom labeling schemes and 50% thermal ellipsoids. Solvent molecule has been omitted for clarity.

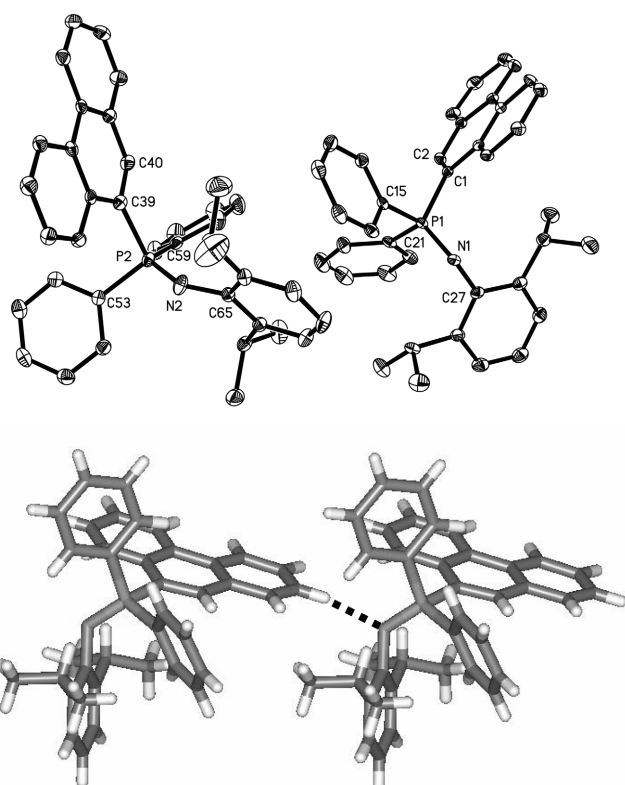


Figure 2. Top: Two molecular structures of **4** along with atom labeling schemes and 30% thermal ellipsoids. All hydrogen atoms have been omitted for clarity. Bottom: Crystal packing diagram of **4** showing the presence of hydrogen bonding between two adjacent molecules.

short wavelengths (blue shift) as going down in the same group from **1** to **3**, which is in agreement with the fact that the change of the reducing strength and the extent of *sp* mixing at the central atoms.¹⁴ The red shift (15–20 nm) in the absorption maximum found in **4** can be explained in terms of the smaller band gap energy as a result of the conjugation of the phosphorus atom with the *N*-arylamine group through the $-P=N-Ar$ bonds. Moreover, π -electrons on the phenanthrenyl group are partially shifted onto the vacant *3d*-

Table 3. Photophysical Data for **1-4**^a

	UV: λ_{max}/nm ($\epsilon/M^{-1}cm^{-1}$)	Em: λ_{max}	Φ_{PL} ^b
1	254 (476030), 301 (124290)	373	0.0252
2	250 (499330), 302 (126330)	366	0.036
3	246 (302790), 297 (73540)	366	0.0153
4	265 (180080), 303 (44740)	373	0.002

^a CH_2Cl_2 solvent at RT with the $[M] = 1.0 \times 10^{-6}$. ^bThe relative quantum yields of PL for all compounds were determined relative to 9,10-diphenylanthracene ($\Phi_{pl} = 0.95$) as the standard in CH_2Cl_2 at 298 K. A range of concentrations of solution of all compounds and standard were measured such that absorbances were less than 0.10 at the excitation wavelength ($\lambda_{ex} = 302$ nm). The quantum yield was then measured by previous known process (ref: Demas, J.N.; Crosby, G. A. *J. Phys. Chem.* 1971, 75, 991).

orbitals of the phosphorus atoms.¹⁵ The compounds **1-3** show purple emission both in solution and as films that were prepared by spin casting methods at room temperature with emission maxima (λ_{max}) at 373, 366, and 366 nm, respectively, attributable to the ligand-centered $\pi \rightarrow \pi^*$ transition in phenanthrene perturbed by the lone pair electrons of the Gps 15 elements. Yet the nature of luminescence observed with **4** differs in that it originates from π (diisopropylbenzene)- π^* (phenanthrene) transitions with the $p\pi$ -contribution from the nitrogen atom. The emission maximum of **4** is red-shifted ranging 350–450 nm due to the internal charge transfer from the phenanthrenyl ring to the *N*-arylamine group as deduced from the *ab initio* calculations.

The so-called heavy-atom effect have recently been observed with some main group organometallic complexes as well incorporating Sb(III) or Bi(III) to reveal efficient phosphorescent emission at low temperature.^{7c} In this regard, one would expect that compounds **2** and **3** exhibit enhanced phosphorescence as compared with **1**, although the measurements could not have been performed due to instrumental limitation. The photoluminescence quantum efficiency were determined relative to 9,10-diphenylanthracene ($\Phi_r = 0.95$), and found to decrease in the following order: **2** (0.03) > **1** (0.02) > **3** (0.01) > **4** (0.002). Thermal

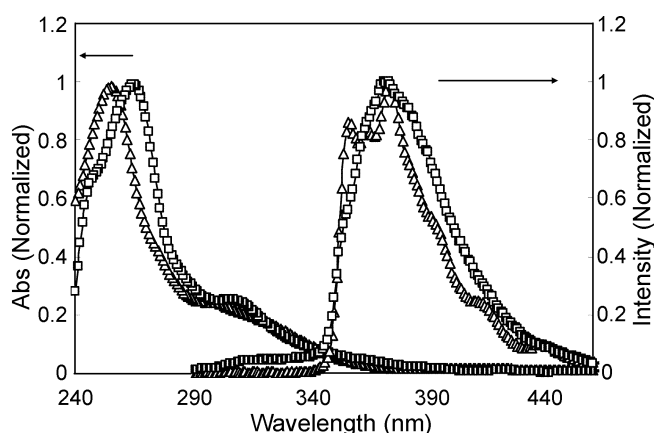


Figure 3. Absorption and emission spectra of **2** (Δ) and **4** (\square) in CH_2Cl_2 .

vibrations caused by Gp 15 elements seem to further induce the loss of energy from the central ions around phenanthrene, thus resulting in such low efficiencies.¹⁶ Of four compounds, the lowest efficiency found with **4** is probably due to the presence of *N*-arylamine which can act as a luminescent quencher.

Molecular Orbital Calculations. To gain a deeper insight into the electronic and luminescent properties of **1-4**, we performed *ab initio* molecular orbital calculations (level of calculation B3LYP/3-21G**) on **2** and **4** employing a Gaussian 98 package.¹⁷ The geometric parameters employed in the calculations were taken from their crystal structural data. A diagram showing the surfaces of HOMO and LUMO along with the orbital energy for each level is depicted in Figure 4. In compound **2**, the HOMO involves π orbitals localized on the phenanthrenyl groups with the contribution from the lone pair orbital of antimony. The LUMO, however, is dominated by the π^* orbitals of phenanthrenyl rings with little contribution from the same central metal. The band gap between HOMO (-5.74 eV) and LUMO (-1.18 eV) is 4.56 eV (271 nm), which is in good agreement

with the optical band gap obtained from the corresponding UV/Vis spectrum (270 nm).¹⁸ Judging from these observations, the luminescence of **2** is believed to originate from ligand-centered transitions (LC) perturbed by the central Sb atom. Such a lone-pair orbital contribution from the central atom in **4** is expected to be negligible, however, where phosphorus is fully oxidized. In fact, the HOMO level of **4** involves π orbitals based on 2,6-diisopropylbenzene with a great contribution from the p_z orbital of nitrogen atom. The band gap between HOMO (-4.95 eV) and LUMO (-1.42 eV) in the ground state of **4** is about 3.53 eV. It can be observed that compound **2** exhibits a wider band gap with lower HOMO and higher LUMO levels relative to **4**. The nature of luminescence observed with **4** originates from π (diisopropylbenzene)- π^* (phenanthrene) transitions with the $p\pi$ -contribution from the nitrogen atom.

Conclusions

We have prepared a series of new group 15 organometallic compounds of the types $\text{M}(\text{phenanthrenyl})_3$ ($\text{M} = \text{P}$ (**1**), Sb (**2**), Bi (**3**)) and $(\text{phenanthrenyl})(\text{Ph})_2\text{P}=\text{N}-(2,6\text{-iPr}_2\text{C}_6\text{H}_3)$ (**4**). Compounds **2** and **4** crystallize with two independent molecules in the asymmetric unit. The compounds **1-3** show purple emission attributable to the ligand-centered $\pi \rightarrow \pi^*$ transition in phenanthrene contributed by the lone pair electrons of the Gp 15 elements. The nature of luminescence observed with **4** differs in that it originates from π (diisopropylbenzene)- π^* (phenanthrene) transitions with the $p\pi$ -contribution from the nitrogen atom. The red shift observed in the emission maximum of **4** is due to the internal charge transfer from the phenanthrenyl ring to the *N*-arylamine group as deduced from the *ab initio* calculations.

Experimental Section

General Remarks. All reactions were carried out under an atmosphere of nitrogen using the standard Schlenk

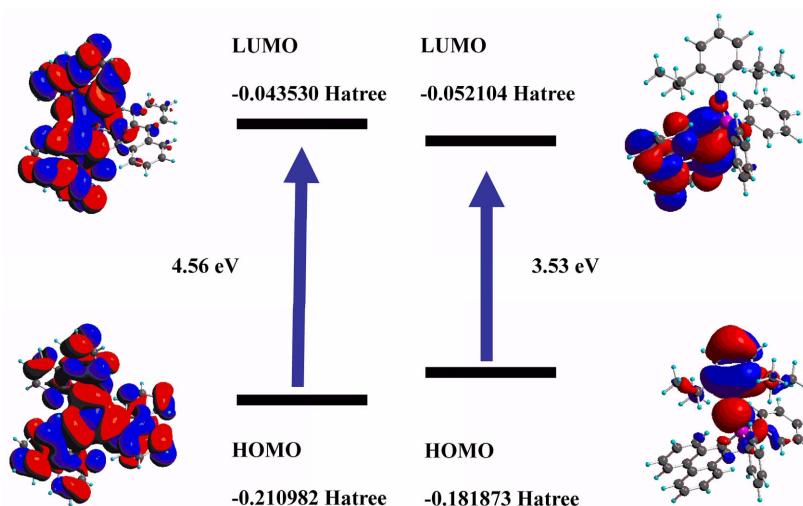


Figure 4. Diagrams of the surfaces and energies of HOMO and LUMO for **2** (left) and **4** (right).

techniques. Solvents were dried using standard procedures. All commercial reagents were purchased from Aldrich and used as received. 2,6-bis(isopropyl)benzoyl azide was prepared according to the literature method.¹⁹

Measurements. The ¹H and ¹³C NMR experiments were performed on a Bruker Advance 400 or 500 Spectrometer by Korea Basic Science Institute (KBSI). The ³¹P NMR spectra were recorded on a Varian Unity Invoxa 300 WB Spectrometer. Chemical shifts were given as δ values with reference to tetramethylsilane (TMS) as an internal standard. Coupling constants are in Hz. GC-Mass spectra were obtained by using a Micromass QUATTRO II GC8000 series model with electron energy of 20 or 70 eV. IR spectra were run on a Mattson FT-IR Galaxy 6030E spectrophotometer by KBSI. UV/Vis and photoluminescent spectra for all samples with concentrations in the range of 10–50 μ M were obtained with a Lambda 900 UV/Vis spectrometer and a Perkin-Elmer Luminescence spectrometer LS 50B. All solutions for photophysical experiments were degassed with more than three repeated freeze-pump-thaw cycles in a vacuum line. Elemental analyses were performed by Center for Instrumental Analysis, Kyungpook National University.

X-ray Crystallographic Analyses. Single crystals of **2** and **4** suitable for X-ray diffraction analyses were obtained by slow diffusion of hexane into a dichloromethane solution containing each compound. The crystals of **2** or **4** were attached to a glass fiber and mounted on a Bruker SMART diffractometer equipped with a CCD-1000 detector and a graphite-monochromated Mo-K α ($\lambda = 0.71073$ Å) radiation, operating at 50 kV and 30 mA; 45 frames of two-dimensional diffraction images were collected and processed to obtain the cell parameters and orientation matrix. All data collections were performed at 173 K. The data collection range over 2θ is 2.14–56.58° for **2** and 2.12–56.62° for **4**, respectively. No significant decay was observed during data collection. The raw data were processed to give structure factors using the SAINT program. Each structure was solved by direction methods and refined by full-matrix least squares against F^2 for all data using the SHELXTL software (version 5.10).²⁰ All non-hydrogen atoms in compounds **2** and **4** were anisotropically refined. All other hydrogen atoms were included in the calculated positions and their contributions in structural factor calculations were included. There are two independent molecules in the asymmetric unit of both compounds. For compound **2**, the half of a solvent molecule (CH₂Cl₂) was found and modeled successfully. Their contribution was also included in the structure factor. The crystals of **2** belong to triclinic crystal system of space group $P1$ while the crystals of compound **4** belong to monoclinic space group $C2/c$. Crystallographic data for **2** and **4** are depicted in Table 1. The ranges of selected bond lengths and angles are given in Table 2. The crystal structures of **2** and **4** along with the atomic-numbering schemes used in refinement are presented in Figures 1 and 2, respectively. Detailed crystal and experimental data are available in Supporting Information.

Quantum Efficiency Measurements. Emission quantum

efficiency of compounds **1–4** were determined relative to 9,10-diphenylanthracene in THF or CH₂Cl₂ at 298 K ($\Phi_{\text{pl}} = 0.95$).

(Phenanthrenyl)₃P (1). To a solution of 9-bromophenanthrene (1.0 g, 3.9 mmol) in hexane (20 mL) in a Schlenk tube at –78 °C was added *n*-BuLi (3.8 mL, 5.8 mmol). After stirring 30 min at –78 °C, the reaction mixture was warmed to room temperature and stirred for an additional 3 h. An ethereal solution (5 mL) of PCl₃ (0.11 mL, 1.3 mmol) was then added through a pressure-equalizing dropping funnel. The resulting suspension was further stirred for 3 h and hydrolyzed with water. The organic layer was extracted, and solvents removed to leave an oily residue. Chromatographic separation on silica gel with a mixture of hexane and ethyl acetate (9 : 1) followed by crystallization from CH₂Cl₂ and hexane afforded a white solid (0.48 g, 66%). ³¹P NMR (CDCl₃, H₃PO₄): δ –28.7 (s). ¹H NMR (CDCl₃): δ 8.80–8.64 (m, 9H), 7.87–7.44 (m, 18H). MS (EI, m/z): Calcd for C₄₂H₂₇P: 562.19. Found: 562.20. Anal. Calcd for C₄₂H₂₇P•(1/2)CH₂Cl₂: C, 84.36; H, 4.66. Found: C, 84.65; H, 4.58.

(Phenanthrenyl)₃Sb (2). This compound was prepared in the same manner as described above replacing PCl₃ with SbCl₃ as a reagent. Yield: 0.58 g, 68%. Off-white single crystals suitable for X-ray structural determination were grown by slow diffusion of hexane into a solution of **2** in CH₂Cl₂. ¹H NMR (CDCl₃): δ 8.80 (d, $J = 9$, 3H), 8.88 (dd, $J = 9$, 3H), 7.77 (s, 3H), 7.68–7.37 (m, 15H). MS (EI, m/z): Calcd for C₄₂H₂₇Sb: 652.12. Found: 652.10. Anal. Calcd. for C₄₂H₂₇Sb•(1/2)CH₂Cl₂: C, 73.31; H, 4.06. Found: C, 73.51; H, 3.87.

(Phenanthrenyl)₃Bi (3). This compound was prepared in the same manner as described above replacing PCl₃ with BiCl₃ as a reagent. Yield: 0.61 g, 63%. ¹H NMR (CDCl₃): δ 8.83 (d, $J = 9$, 3H), 8.70 (d, $J = 9$, 3H), 8.39 (s, 3H), 8.22 (dd, $J = 9$, 3H), 7.68–7.32 (m, 15H). MS (EI, m/z): Calcd for C₄₂H₂₇Bi: 740.19. Found: 740.20. Anal. Calcd. for C₄₂H₂₇Bi•(1/2)CH₂Cl₂: C, 65.18; H, 3.60. Found: C, 65.41; H, 3.61.

(Phenanthrenyl)(Ph)₂P(=N-2,6-ⁱPr₂-C₆H₃) (4). To a stirring solution of 9-(diphenylphosphino)phenanthrene (1.0 g, 2.8 mmol) in THF (15 mL) was added 2,6-diisopropylphenyl azide (1.1 g, 5.5 mmol). The mixture was stirred for 5 h, after which all volatiles were removed under vacuum. The remaining oily yellow solid was washed several times with hexane and dissolved in a mixture of CH₂Cl₂ and hexane (1 : 4) for crystallization. The product was obtained as yellow single crystals suitable for X-ray structural determination. Yield: 1.2 g, 87%. ³¹P NMR (CDCl₃, H₃PO₄): δ –4.04 (s). ¹H NMR (CDCl₃): δ 0.66 (d, $J = 6.6$, 12H), 3.25 (m, 2H), 6.75 (br, 1H), 6.86 (d, $J = 6.0$, 2H), 7.26–7.75 (m, 17H), 8.59 (d, $J = 8.1$, 1H), 8.70 (d, $J = 8.1$, 1H). MS (EI, m/z): Calcd for C₃₈H₃₆NP: 537.67. Found: 537.65. Anal. Calcd. for C₃₈H₃₆NP: C, 84.89; H, 6.75. Found: C, 84.73; H, 6.79.

Acknowledgment. This work was supported by a grant from The Advanced Medical Technology Cluster for Diagnosis and Prediction at KNU from MOCIE, ROK.

Supporting Information Available: Absorption and emission spectra of **1-4**, and tables giving atomic coordinates, displacement parameters, and bond distances and angles for **2** and **4**. This material is available at <http://www.kcsnet.or.kr/bkcs> or from the author.

References

- (a) Tang, C. W.; VanSlyke, S. A. *Appl. Phys. Lett.* **1987**, *51*, 913. (b) Tang, C. W.; VanSlyke, S. A.; Chen, C. H. *J. Appl. Phys.* **1989**, *65*, 3610. (c) Hu, N.-X.; Esteghamatian, M.; Xie, S.; Popovic, Z.; Ong, B.; Hor, A. M.; Wang, S. *Adv. Mater.* **1999**, *11*, 1460. (d) Bulovic, V.; Gu, G.; Burrows, P. E.; Forrest, S. R.; Thompson, M. E. *Nature* **1996**, *380*, 29. (e) Balzani, V.; Juris, A.; Venturi, M.; Campagna, S.; Serroni, S. *Chem. Rev.* **1996**, *96*, 759. (f) Shen, Z.; Burrows, P. E.; Bulovic, V.; Forrest, S. R.; Thompson, M. E. *Science* **1997**, *276*, 2009. (g) Papkovski, D. B. *Sens. Actuators, B* **1995**, *29*, 213. (h) Ma, Y.; Che, C.-M.; Chao, H.-Y.; Zhou, X.; Chan, W.-H.; Shen, J. *Adv. Mater.* **1999**, *11*, 852. (i) Mills, A.; Lepre, A. *Anal. Chem.* **1997**, *69*, 4653. (j) Poterini, G.; Serpone, N.; Bergkamp, M. A.; Netzel, T. L. *J. Am. Chem. Soc.* **1983**, *105*, 4639. (k) Ma, Y.; Zhang, H.; Shen, J.; Che, C.-M. *Synth. Met.* **1998**, *94*, 245. (l) Baldo, M. A.; Thompson, M. E.; Forrest, S. R. *Nature* **2000**, *403*, 750. (m) Papkovski, D. B.; Ponomarev, G. V.; Kurochkin, I. N.; Korpela, T. *Anal. Lett.* **1995**, *28*, 2027.
- (a) Baldo, M. A.; O'Brien, D. F.; You, Y.; Shoustikov, A.; Sibley, S.; Thompson, M. E.; Forrest, S. R. *Nature* **1998**, *395*, 151. (b) Adachi, A.; Baldo, M. A.; Forrest, S. R.; Lamansky, S. M.; Thompson, E. R.; Kwong, C. *Appl. Phys. Lett.* **2001**, *78*, 1622. (c) Adachi, A.; Kwong, R. C.; Djurovich, P.; Adamovich, V.; Baldo, M. A.; Thompson, M. E.; Forrest, S. R. *Appl. Phys. Lett.* **2001**, *79*, 2082. (d) O'Brien, D. F.; Baldo, M. A.; Thompson, M. E.; Forrest, S. R. *Appl. Phys. Lett.* **1999**, *74*, 442. (e) Baldo, M. A.; Lamansky, S.; Burrow, P. E.; Thompson, M. E.; Forrest, S. R. *Appl. Phys. Lett.* **1999**, *75*, 4. (f) Kwong, R. C.; Sibley, S.; Dubovoy, T.; Baldo, M.; Forrest, S. R.; Thompson, M. E. *Chem. Mater.* **1999**, *11*, 3709. (g) Thompson, M. E.; Burrow, P. E.; Forrest, S. R. *Curr. Opin. Solid State Mater. Sci.* **1999**, *4*, 369. (h) Lamansky, S.; Djurovich, P.; Murphy, D.; Abdel-Razzag, F.; Lee, H.-E.; Adachi, C.; Burrows, P. E.; Forrest, S. R.; Thompson, M. E. *J. Am. Chem. Soc.* **2001**, *123*, 4304. (i) Lamansky, S.; Djurovich, P.; Murphy, D.; Abdel-Razzag, F.; Kwong, R.; Tsyba, I.; Bortz, M.; Mui, B.; Bau, R.; Thompson, M. E. *Inorg. Chem.* **2001**, *40*, 1704. (j) Sprouse, S.; King, K. A.; Spellane, P. J.; Watts, R. J. *J. Am. Chem. Soc.* **1984**, *106*, 6647. (k) Baldo, M. A.; Thompson, M. E.; Forrest, S. R. *Pure Appl. Chem.* **1999**, *71*, 2095.
- (a) Wu, Q.; Esteghamatian, M.; Hu, N.-X.; Popovic, Z.; Enright, G.; Tao, Y.; D'Iorio, M.; Wang, S. *Chem. Mater.* **2000**, *12*, 79. (b) Wu, Q.; Esteghamatian, M.; Hu, N.-X.; Popovic, Z.; Enright, G.; Breeze, S. R.; Wang, S. *Angew. Chem., Int. Ed.* **1999**, *38*, 985. (c) Pang, J.; Tao, Y.; Freiberg, S.; Yang, X. P.; D'Iorio, M.; Wang, S. *J. Mater. Chem.* **2002**, *12*, 206. (d) Pang, J.; Marotte, E. J. P.; Seward, C.; Brown, R. S.; Wang, S. *Angew. Chem., Int. Ed.* **2001**, *40*, 4042.
- (a) Baldo, M. A.; Thompson, M. E.; Forrest, S. R. *Nature* **2000**, *403*, 750. (b) Kwong, R. C.; Sibley, S.; Dubovoy, T.; Baldo, M. A.; Forrest, S. R.; Thompson, M. E. *Chem. Mater.* **1999**, *11*, 3709. (c) Kwong, R. C.; Lamansky, S.; Thompson, M. E. *Adv. Mater.* **2000**, *12*, 1134. (d) Lamansky, S.; Djurovich, P.; Murphy, D.; Abdel-Razzag, F.; Lee, H.-E.; Adachi, C.; Burrows, P. E.; Forrest, S. R.; Thompson, M. E. *J. Am. Chem. Soc.* **2001**, *123*, 4304. (e) Lamansky, S.; Djurovich, P.; Murphy, D.; Abdel-Razzag, F.; Kwong, R. C.; Tsyba, I.; Bortz, M.; Mui, B.; Bau, R.; Thompson, M. E. *Inorg. Chem.* **2001**, *40*, 1704.
- (a) Pomestchenko, I. E.; Luman, C. R.; Hissler, M.; Zissel, R.; Castellano, F. N. *Inorg. Chem.* **2003**, *42*, 1394. (b) Brooks, J.; Babayan, Y.; Lamansky, S.; Djurovich, P.; Tsyba, I.; Bau, R.; Thompson, M. E. *Inorg. Chem.* **2002**, *41*, 3055. (c) Duan, J. P.; Sun, P. P.; Chen, C. H. *Adv. Mater.* **2003**, *15*, 224. (d) Chen, F. C.; He, C. F.; Yang, Y. *Appl. Phys. Lett.* **2003**, *82*, 1006. (e) Adachi, C.; Baldo, M. A.; Thompson, M. E.; Forrest, S. R. *J. Appl. Phys.* **2001**, *90*, 5048.
- (a) Lakowicz, J. R. *Principles of Fluorescence Spectroscopy*, 2nd ed.; Kluwer Academic: New York, 1999. (b) Ingle, J. D.; Crouch, S. R. Jr. *Spectrochemical Analysis*; Prentice Hall: Englewood Cliffs, NJ, 1988; Chapter 12.
- (a) Hassan, A.; Breeze, S. R.; Courtenay, S.; Deslippe, C.; Wang, S. *Organometallics* **1996**, *15*, 5613. (b) Wu, S. Q.; Lavigne, J. A.; Tao, Y.; D'Iorio, M.; Wang, S. *Chem. Mater.* **2001**, *13*, 71. (c) Kang, Y.; Song, D.; Schmider, H.; Wang, S. *Organometallics* **2002**, *21*, 2413. (d) Jia, W.-L.; Liu, Q.-D. R.; Wang, S. *Organometallics* **2003**, *22*, 4070. (e) Lee, J.; Liu, Q.-D.; Motala, M.; Dane, J.; Gao, J.; Kang, Y.; Wang, S. *Chem. Mater.* **2004**, *16*, 1869. (f) Jia, W.-L.; Bai, D.-R.; McCormick, T. M.; Liu, Q.-D.; Motala, M.; Wang, R.-Y.; Seward, C.; Tao, Y.; Wang, S. *Chem. Eur. J.* **2004**, *10*, 994.
- (a) Kim, T.-J.; Kim, D.-U.; Paik, S.-H.; Kim, S.-H.; Tak, S.-H.; Han, Y.-S.; Kim, K.-B.; Ju, H.-J. *Materials Science and Engineering: C* **2004**, *24*, 147. (b) Kim, K.-D.; Han, Y.-S.; Tak, Y.-H.; Kim, D.-U.; Kim, T.-J.; Yoon, U.-C.; Kim, S.-H.; Moon, H.-W. *European Patent No.* 03027185.2 (EU), 2004, 01. 20.
- Phosphorus: The Carbon Copy*; Dillon, K. B.; Mathey, F.; Nixon, J. F., Eds; John Wiley and Sons: New York, 1998.
- Nyulaszi, L.; Veszpremi, T.; Reffy, J. *J. Phys. Chem.* **1993**, *97*, 4011.
- Wright, V. A.; Gates, D. P. *Angew. Chem. Int. Ed.* **2002**, *41*, 2389.
- For a recent example employing a ligand similar to our system, see: Cadierno, V.; Diez, J.; Garcia-Alvarez, J.; Gimono, J. *Organometallics* **2004**, *23*, 2421.
- Chandross, E. A.; Thomas, H. T. *J. Am. Chem. Soc.* **1972**, *94*, 2421.
- Vogler, A.; Paukner, A.; Kunkely, H. *Coord. Chem. Rev.* **1990**, *97*, 285.
- Razuvaev, G. A.; Egorochkin, A. N.; Kuznetsov, V. A.; Glushakova, V. N.; Shabanov, A. V. *J. Organomet. Chem.* **1978**, *148*, 147.
- Fluorescence and Phosphorescence*; Rendell, D., Ed.; John Wiley & Sons: New York, 1987.
- Frisch, M. J.; Trucks, G. W.; Schlegel, H. B.; Scuseria, G. E.; Robb, M. A.; Cheeseman, J. R.; Zakrzewski, V. G.; Montgomery, J. A., Jr.; Stratmann, R. E.; Burant, J. C.; Dapprich, S.; Millam, J. M.; Daniels, A. D.; Kudin, K. N.; Strain, M. C.; Farkas, O.; Tomasi, J.; Barone, V.; Cossi, M.; Cammi, R.; Mennucci, B.; Pomelli, C.; Adamo, C.; Clifford, S.; Ochterski, J.; Petersson, G. A.; Ayala, P. Y.; Morokuma, Q. K.; Malick, D. K.; Rabuck, A. D.; Raghavachari, K. J.; Cioslowski, B. J.; Ortiz, J. V.; Stefanov, B. B.; Liu, G.; Liashenko, A.; Piskorz, P.; Komaromi, I.; Gomperts, R.; Martin, R. L.; Fox, D. J.; Keith, T.; Al-Laham, M. A.; Peng, C. Y.; Nanayakkara, A.; Gonzalez, C.; Challacombe, M.; Gill, P. M. W.; Johnson, B. G.; Chen, W.; Wong, M. W.; Andres, J. L.; Head-Gordon, M.; Replogle, E. S.; Pople, J. A. *Gaussian 98*, revision A.6; Gaussian, Inc.: Pittsburgh, PA, 1998.
- The weak band found at longer wavelength has a triplet (T1) character, which explains a slight mismatch between the UV-edge (experimental data) and the band gap (theoretical value). The calculations performed by employing the time dependent-density function theory (TD-DFT) reveal the T1-excitation energies of 440 nm (2.81 eV) and 370 nm (3.33 eV) for **2** and **4**, respectively.
- Spencer, L. P.; Altwer, R.; Wei, P.; Gelmini, L.; Gauld, J.; Stephan, D. W. *Organometallics* **2003**, *22*, 3841.
- SHELXTL NT Crystal Structure Analysis Package*, Version 5.10; Bruker AXS, Analytical X-ray System, Madison, WI, 1999.